ELSEVIER

Journal of Hazardous Materials 46 (1996) 117–129

JOURNAL OF HAZARDOUS MATERIALS

Full-scale depressurization of a section of a riser platform. Measurements and comparison with simulations

T. Evanger[a], T. Bjørge[a,*], B.F. Magnussen[a], A. Bratseth[b]

[a] *SINTEF/NTH, Applied Thermodynamics, Trondheim, Norway*
[b] *STATOIL, Stavanger, Norway*

Received 29 April 1994; accepted 27 January 1995

Abstract

Full-scale depressurization tests have been carried out on a riser platform in order to measure outer surface temperatures in the depressurized section of the platform. The tests are performed primarily to find out if the occurring steel temperatures are acceptable during depressurization, and secondly to obtain full-scale experimental data for comparison with the simulation code PIA. Blow-down from two initial pressure levels were tested, 88 and 70 bar. The test section volume was depressurized through a 25 mm nozzle and a pressure of 8 bar was obtained after about 11 and 9 min, respectively. The results of the measurements show that the maximum surface temperature drop is about 9 °C at an initial pressure of 88 bar and 6 °C at an initial pressure of 70 bar. The lowest outer surface temperature registered was − 4 °C. The depressurization tests were also simulated using the finite difference code PIA, and the results for outer wall temperatures are in close agreement with the measurements. Comparisons between heat transfer coefficients used in the simulation code and estimated heat transfer coefficients from the measurements are also in good agreement.

Keywords: Safety; Process technology; Depressurization; Simulations; Measurements

1. Introduction

During emergency situations on gas processing plants or on oil and gas platforms, the pressure of the installation must be reduced to avoid possible accidents. This is mostly done by discharging the gas to a flare system. The depressurization of the, relatively, low-temperature gas from high pressure (may be more than 100 bar) to low pressure during a limited time causes large temperature decreases in the gas in the

* Corresponding author. Fax: + 477359 3580. Tel.: 4773593844.

SSDI 0304-3894(95)00064-X

piping system, tanks, etc. This could represent a safety problem if the lower-temperature limit of the material (steel) is reached. In addition, situations could emerge in which a fire is developing in the vicinity of high-pressure equipment and a blow-down of the installation could then cause extensive thermal stresses in the steel due to a high outer wall temperature (radiation from the fire) and a low inner wall temperature. From a safety point of view, it is therefore important in the design phase to analyse the behaviour of process equipment during depressurization for different emergency situation scenarios.

This can be achieved using a CFD code developed for the purpose of simulating blow-down of process equipment in hazardous environments. Such a code should incorporate realistic models concerning the gas properties (real gas behaviour), heat transfer coefficients and thermal stresses. The code should also be validated against experimental data when possible. This paper reports measurements on depressurization of parts of the topside piping on a riser platform in operation and the results are compared with the results of simulations using the CFD code PIA, which is designed especially for this purpose.

2. Measurements

2.1. Equipment

The depressurization tests were performed measuring outside wall temperatures, gas temperatures and gas pressures. The outside wall temperatures were obtained using bare thermocouples type K of 0.2 mm thickness which were made flat to a thickness of 0.18 mm. These thermocouples were attached to the outer pipe wall using Loctite Black Max 380 cyanoacrylic glue. This method of attaching the thermocouples were tested and showed that the discrepancy between a thermocouple mounted in a groove in the surface and a thermocouple glued to the surface was about 0.2 °C at 1.5 °C surface temperature and 0.5 °C at −18 °C surface temperature. The reference temperature during the measurements is 0 °C (finely crushed ice/water).

The gas temperature measurements were performed using thermocouples of type K upstream and downstream of the mass flow controlling nozzle. This nozzle was inserted to get a blow-down duration of about 12 min. The nozzle had a diameter of 25 mm and had a rounded inlet and the nozzle coefficient should be from 0.96 to 0.98 [1] although this was not measured. The nozzle coefficient is here assumed to be 0.96. The reference temperature during the measurements is again 0 °C. In addition, the gas temperature was measured in the pipe system using an existing temperature transmitter-type Rosemount 444-RL9-U-1-A218 with a measuring region of −100 °C to +100 °C. This transmitter has an output of 4–20 mA which is converted to 0.4–2 V by passing the signal through a 100 Ω resistance. The gas pressure was measured at three different positions using pressure transducers of type Foxboro 841 GM-EI1, CS-E/PB-E with a range of 0–165 bar. The transducers have an output of 4–20 mA which again is converted to 0.4–2 V by passing the signal through a 100 Ω resistance.

The gas pressure is measured upstream and downstream of the nozzle and at the far end of the depressurized pipe system.

The thermocouples/transmitters are connected to separate A/D converters in groups of 12 through short cables. This to avoid the use of amplifiers. The A/D converters are Schlumberger 35951A isolated measurement pods (IMP). These A/D converters have 20 channels [2]. In order to make the measurement equipment Ex approved, each IMP was placed in a EEx de (ia) IIC T5 housing. The IMPs are connected in series to a PC by a S-Net cable. The total cable length can be up to 1000 m. To control the IMPs, a PC to S-Net Adaptor is located in the PC [3] (Schlumberger 35954A). The voltage supply to the IMPs goes through the S-Net cable using an external voltage supply (Schlumberger 359595A). The last IMP has a termination at the S-Net output to prevent reflections in the S-Net cable. The data collection is controlled by the Altair software from Dickinson Control System Ltd. [4]. Further data analysis is performed using the Cypros software [5].

2.2. Location of surface temperature measurement points

The section of the riser platform subject to blow-down consisted of pipes of different size as shown in Table 1. The weight of the valves limiting the gas volume is about 46 700 kg. The total gas volume is 24.87 m^3 and this volume determines the mass of gas before depressurization. The pipe system and the location of the surface temperature measurement cross-sections are shown in Fig. 1. There are nine measurement cross-sections on the pipe system each consisting of a number of thermocouples as shown in Fig. 2 and Table 2.

2.3. Gas composition

The gas used in the test is as given in Table 3 with a molecular weight of 18.38 kg/kmol.

Table 1
Geometrical data for the pipe system

Pipe diameter (")	Pipe length (m)	Outer diameter (mm)	Inner diameter (mm)	Wall thickness (mm)	Gas volume (m^3)	Steel mass (kg)
36	15.91	961.44	870.00	45.72	9.46	18361
30	38.90	762.00	688.30	36.83	14.47	25635
14	9.59	355.60	314.96	20.32	0.75	2813
8	8.73	291.10	193.70	12.70	0.18	1514
2	5.50	60.30	49.22	5.54	0.0105	63

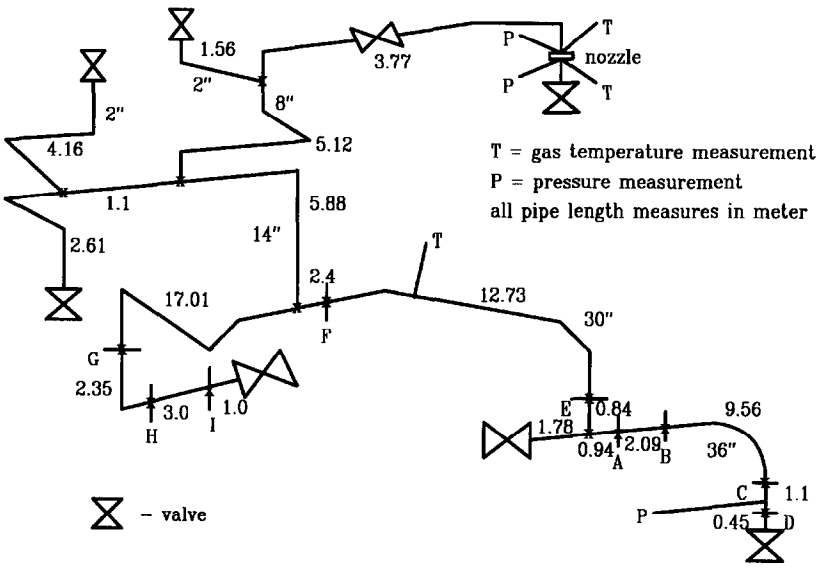

Fig. 1. Pipe system with surface temperature measurement cross-sections, gas temperature measurement points and pressure measurement points.

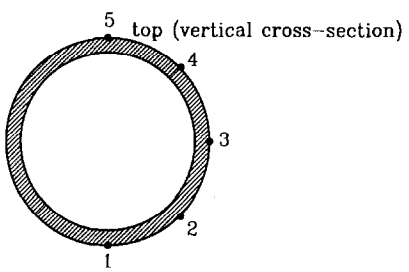

Fig. 2. Position of measurement points in a measurement cross-section.

3. Simulations

3.1. Calculation model

For the numerical calculations the program system PIA, developed at NTH/SINTEF Division Thermodynamics, has been used. PIA [6] is a program system designed for analysis of the behaviour of process equipment, also in hazardous environments like extensive fires, during blow-down. PIA is based on finite difference technique for numerical calculation of general heat and mass transfer both in fluid and solid material. It is linked to an extensive thermodynamic program package for equilibrium calculations and for calculation of multicomponent hydrocarbon

Table 2
Position of measurement points in each surface temperature measurement cross section

Cross section	Point No.					Cross sectional orientation
	1	2	3	4	5	
A	×	×	×		×	Vertical
B	×	×	×		×	Vertical
C	×	×	×	×	×	Horizontal
D	×	×	×	×	×	Horizontal
E			×	×	×	Horizontal
F	×	×	×	×	×	Vertical
G	×	×	×	×	×	Horizontal
H	×	×	×		×	Vertical
I	×	×	×		×	Vertical

Table 3
Gas composition

Component	N_2	CO_2	C1	C2	C3	*n*C4	*i*C4	*n*C5	*i*C5	C6 +
Mol %	0.81	0.34	88.70	6.31	2.82	0.30	0.51	0.071	0.074	0.065

properties, and it includes optional calculation of thermal stresses caused by temperature gradients in the solid material. A combination of 1D fluid flow grid and 2D wall grid is used.

In axial direction a nonuniform grid consisting of 15 grid points for each pipe element is used, and in radial direction 6 nodes through the solid wall is applied. For a controlled blow-down the axial gradients are rather small in the pressurized sections of the equipment, and the radial heat transfer conditions are in general more important. In general, heat transfer in both fluid and in solid in PIA are calculated by solution of the basic conservation equation for enthalpy:

$$\frac{\partial}{\partial t}(\rho h) + \frac{\partial}{\partial x_j}(\rho u_j h) = \frac{\partial}{\partial x_j}\left(\Gamma_h \frac{\partial h}{\partial x_j}\right) + S_h, \tag{1}$$

where ρ is the density, h is the enthalpy, u_j is the velocity, Γ_h is the transport coefficient and S_h is a source term. The heat transfer between the solid wall and the surroundings and between the wall and the gas, form parts of the source term S_h for boundary control volumes:

$$S_h = \frac{q}{V} = h_i A \frac{\Delta T}{V}, \tag{2}$$

where q is the heat transfer rate, V is the volume of the control volume, h_i is the heat transfer coefficient, A is the heat transfer area and ΔT is the temperature difference. At

the outer and inner surface of the pipe-work the heat transfer coefficients are calculated by use of conventional correlations. As the surrounding air flow is not included in the simulations the external heat transfer coefficient h_∞ is kept constant, $h_\infty = 10\ \mathrm{W/m^2\ K}$. This is taken as a mean value because the heat transfer coefficient on the outside of the pipe is between 3 and 27 $\mathrm{W/m^2\ K}$ depending on whether the pipe is exposed to the wind or not. The internal heat transfer coefficient is dependent on the actual flow situation, and in PIA different correlations are implemented to cover a number of different flow situations. The program selects correlations either for natural, mixed or forced convection based on the Grashof and Reynolds numbers [7], and in the present study natural convection is the dominant internal heat transfer mode. The following correlations for natural convection has been applied [6, 7]:

$$
\begin{aligned}
Nu_L &= 0.046(Gr_L Pr)^{0.33}, \quad 10^6 < Gr_L Pr < 10^9,\\
Nu_D &= 0.55(Gr_D Pr)^{0.25}, \quad L/D < 2,\\
Nu_D &= 0.59(Gr_D Pr)^{0.25}, \quad 10^4 < Gr_D Pr < 10^9,\\
Nu_D &= 0.13(Gr_D Pr)^{0.33}, \quad 10^9 < Gr_D Pr < 10^{12},\\
Nu_D &= 4.69 Re_D^{0.27} Gr^{0.07} (D/L)^{0.36}.
\end{aligned} \tag{3}
$$

The properties for the steel are taken as typical carbon steel values which are: a density of $7800\ \mathrm{kg/m^3}$, a thermal conductivity of $50\ \mathrm{W/m\,K}$ and a specific heat capacity of $500\ \mathrm{J/kg\,K}$. The fluid flow calculations are 1D in axial direction, implying that heat transfer calculations are based on bulk conditions at each cross-section (control volume). During depressurization of gas systems condensation may take place. The condensation rate and the amount of liquid generated are calculated within each control volume at each time level by flash calculations assuming equilibrium conditions at each time level. For the fluid flow a two-phase situation is approached by using a homogeneous two-phase model. A homogeneous approach is also used for the heat transfer calculations. Local effects like spot cooling caused by droplet evaporation on internal wall surfaces with temperature above the boiling temperature for the mixture, is thus not taken into consideration with the present model. Neither is the different heat transfer conditions that could occur at the inner surface of a horizontal pipe containing liquid as a separate phase wetting parts of the internal surface or as a liquid film.

3.2. Geometrical model of the test section

The test section consists of parts of the riser topside piping as described in Fig. 1. The numerical model is however simplified and limited to the 30″ and 36″ carbon steel pipes as these are the most critical ones regarding low steel temperatures. The 14″ pipe, the 8″ pipe and the 2″ pipes are of a higher steel quality with lower temperature limits. A sketch of the simulation system is shown in Fig. 3. The location of the 9 measurement cross-sections, A-I, defined in Table 2 and Fig. 1 are also indicated in the figure. The outlet flow rate is calculated as critical single-phase flow. The critical properties including the speed of sound are calculated for the real gas mixture by the

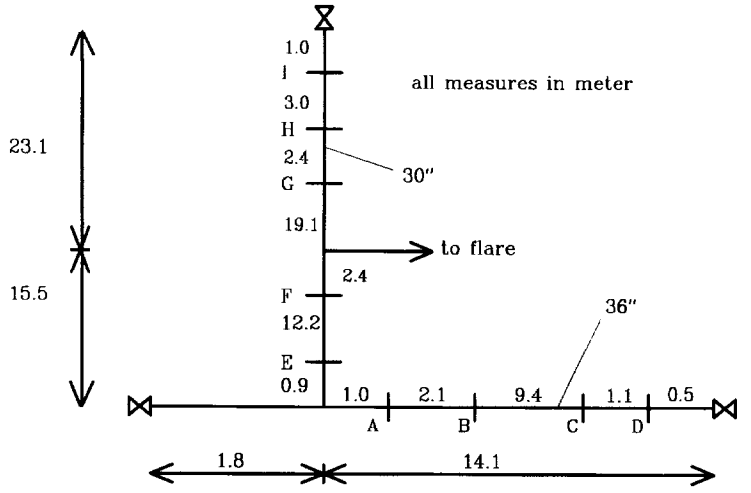

Fig. 3. Sketch of the numerical geometry model of the blow-down system.

thermodynamic package. The effective orifice area is given by the orifice diameter 25 mm and nozzle coefficient 0.96. As the simulation program is 2D for steel temperature calculation (radial and axial direction) the measured temperatures in each cut A-I is averaged for comparison with the calculated temperatures.

4. Results of measurements and simulations

4.1. Initial conditions

Two different test cases were performed. For case I the initial pressure is 88 bar. The initial wall temperature (and probably also the gas temperature) varies throughout the system between 3 and 7 °C. The gas temperature is about 10 °C. However, as sufficient information about the temperature variation throughout the system was not available an average steel temperature of 6 °C is used as initial temperature for the 36″ pipe, and 8 °C for the 30″ pipe for the simulations. Further, the gas temperature was assumed to be 6 °C for the 36″ pipe and 8 °C for the 30″ pipe, equal to the wall temperature, in the simulations. For case II the initial pressure is 70 bar. An initial temperature of 11 °C is used for both the gas and the steel.

4.2. Pressure and mass flow

The pressure and the gas temperature upstream of the nozzle are measured in the 8″ pipe, which is not included in the simulations. However, as the axial pressure gradient is negligible the calculated pressure in the 30″ pipe is compared with the measured pressure for case I in Fig. 4(a). The calculated flow rates based on the calculated pressure and the measured pressure are compared in Fig. 4(b). The results for case II

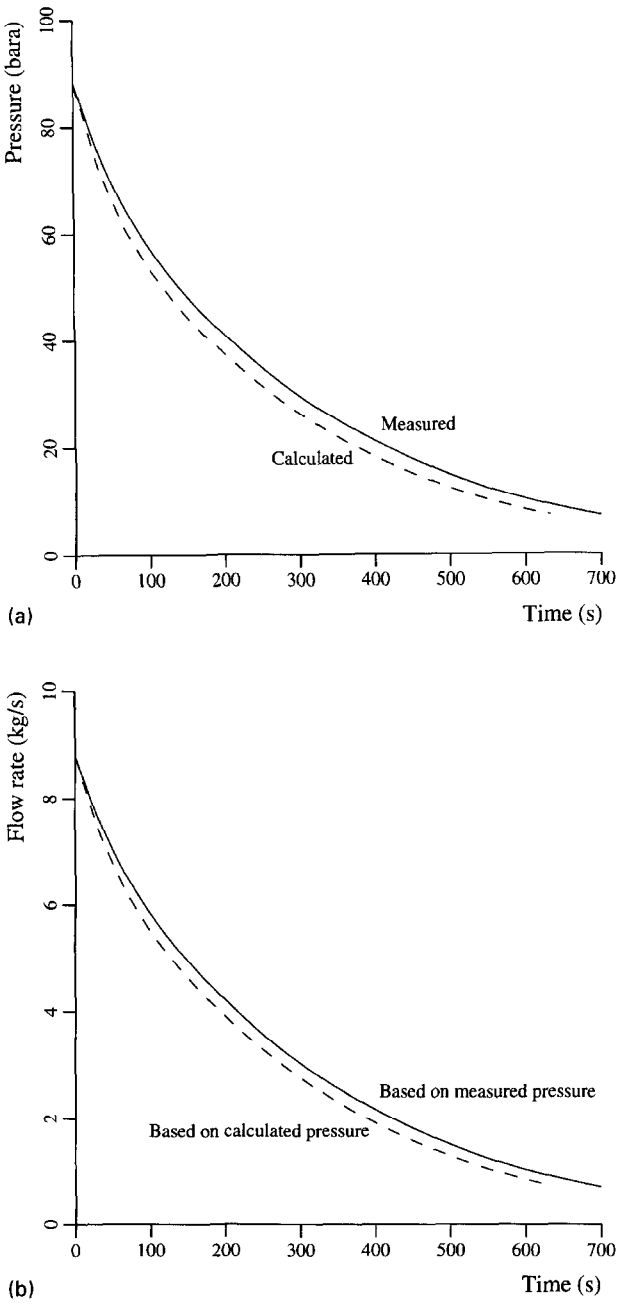

Fig. 4. Comparison of measured and calculated pressure (a) and mass flow based on measured and calculated pressure (b), case I.

were similar to these. As can be seen the calculated results are in accordance with the measured values. However, minor deviations in the calculated and measured pressure and flow rate can be observed and this is caused by (1) the total volume of the calculation domain is less than the real volume as the 14″ and the 8″ pipes are not included and (2) a gas leakage at one of the valves was observed during the tests. The magnitude of the leakage rate is however unknown. A discrepancy of 5–10% in the mass flow should not influence the wall temperatures very much.

4.3. *Surface temperatures*

Results of the measurements and calculations are shown in Fig. 5 and Table 4 for both test cases. The grid node locations in the calculation grid are slightly different from the exact location for the various thermocouples, but this is not regarded to be of significant importance. All the temperature decreases reported in Fig. 5 and Table 4 are mean values of all the measurement points for a cross-section. In cross-sections A, B, F, H and I, two numbers are reported in Table 4 for the measurements. The numbers in parantheses refer to a mean value were the point on top of the pipe (point 5, Fig. 2) is excluded. There is a quite pronounced effect of excluding this point as shown in Table 4. The reason is possibly the formation of a secondary flow in the horizontal pipes, the gas flowing upwards at the hot pipe wall producing a turning point at the top of the cross-section with a layer of stagnant gas (in the cross-stream direction) as a result. This produces a lower heat transfer coefficient which the 2D code is not able to simulate. In PIA flash calculations are performed for each control volume at each time step, and condensed liquid is assumed to be present as mist and is uniformly distributed in the control volume. However, very little liquid is generated during the blow-down. The lowest calculated void fraction is 0.996 after about 3 min (case I). The effect of boiling of liquid droplets at the wall is not included in the simulations and could be a source of error when simulations are compared with measurements. However, the presence of droplets will increase the density and hence the heat transfer coefficient in the simulations. It is therefore not straightforward to evaluate the influence of condensation in the measurements and simulations.

Generally, cross-sections close to valves, T junctions or bends should have a higher heat transfer coefficient than cross-sections in straight pipes due to the developing boundary layer. Admittedly the difference in ΔT is not big, but a trend supporting this is evident from Table 4. In cross-sections D and I (excluding point 5 in I) the assumingly higher heat transfer coefficient in the measurements could be due to the close proximity to the valve and hence thin boundary layer (velocities from 0.2 to 1 m/s during depressurization). This is not included in the simulation.

In cross-section H the difference between measurement and simulation is more pronounced than in the other cross-sections, especially for case I. The reason for this is uncertain, but one explanation could be that this cross-section has the longest straight pipe upstream of all the cross-sections.

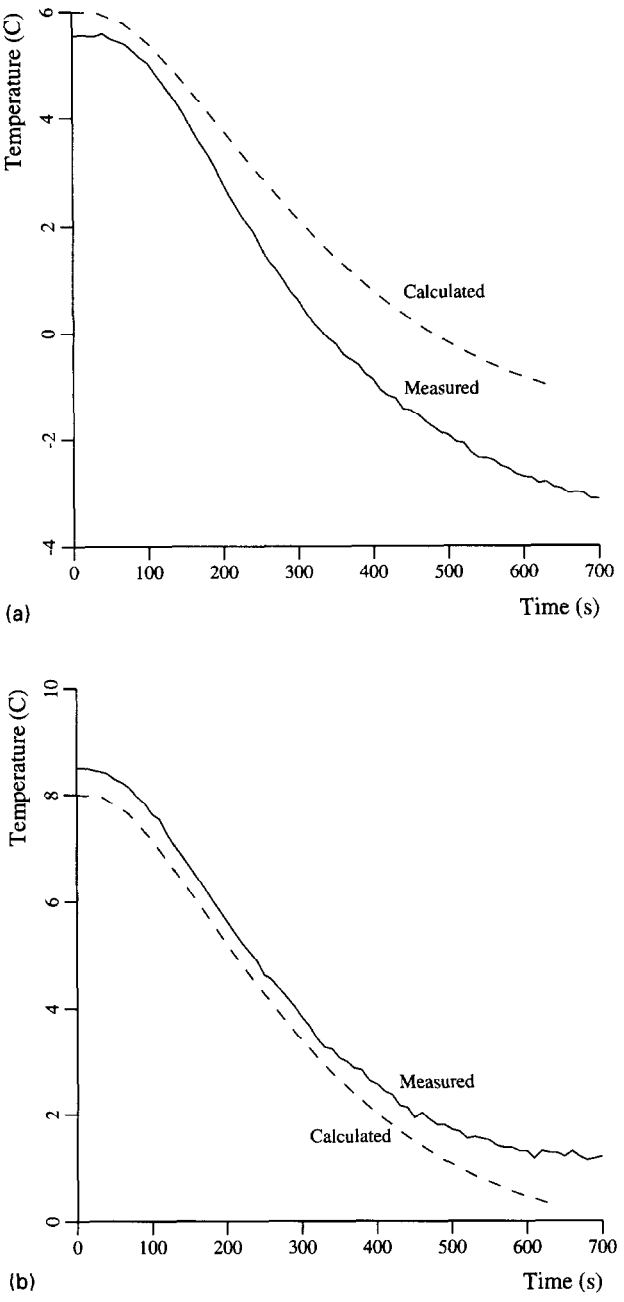

Fig. 5. Comparison of measured and calculated surface temperature for cross-section D (a) and G (b), case I.

Table 4
Comparison of measured and calculated depressurization temperature decreases

Cross-section	Case I ΔT (°C)		Case II ΔT (°C)	
	Measurement	Simulation	Measurement	Simulation
A	6 (7.4)	7.2	4.1 (5.0)	4.9
B	6 (7.4)	7.2	4.4 (5.5)	4.9
C	6.5	7.0	4.8	4.8
D	8.4	7.0	5.3	4.7
E	8.6	9.1	6.2	6.0
F	6.3 (7.3)	8.3	4.4 (5.1)	5.6
G	7.2	7.7	5.5	5.4
H	4.6 (5.4)	7.6	3.6 (4.2)	5.3
I	7.3 (9.0)	7.5	4.8 (5.8)	5.2

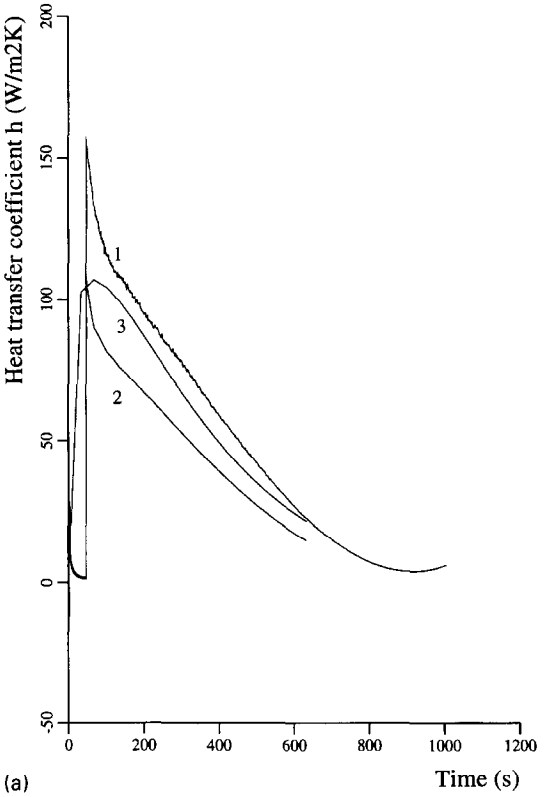

Fig. 6. Estimated heat transfer coefficient h_i based on measured gas temperature at nozzle (1), based on measured gas temperature minus 10 °C (2) and based on calculations by PIA (3). Cross-section G (a) and E (b), case I.

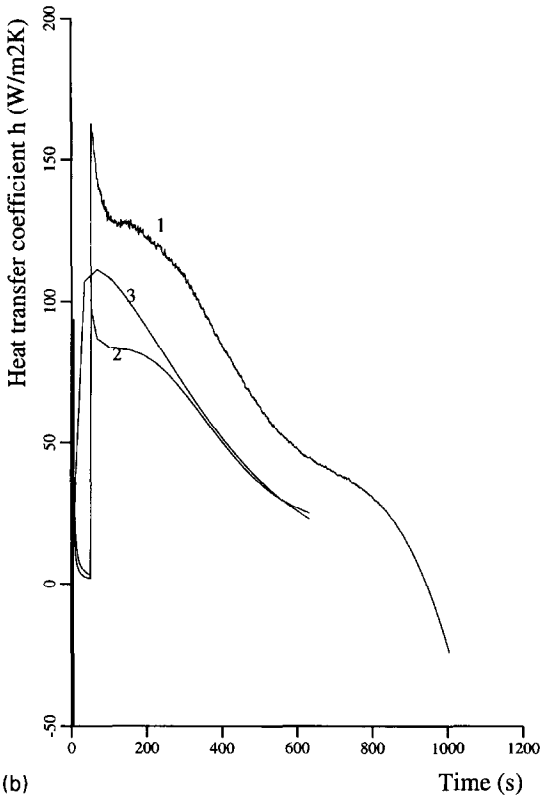

Fig. 6. Continued.

4.4. Heat transfer coefficients

The heat transfer coefficient between the inner pipe wall and the gas, h_i, is estimated from the measured outer wall temperature assuming (1) pure radial heat transfer, (2) constant heat capacity of the pipe, (3) the heat transfer coefficient is 10 W/m^2 K on the outside of the pipe and (4) no temperature gradient in the pipe wall. The temperature gradient through the pipe wall is negligible as long as the Biot number ($Bi = h_i L_c/k_s$) for the inner pipe wall is less than 0.1 [7]. The Biot numbers in these measurements are less than 0.15 (assuming h_i less than 100 W/m^2 K) and assumption (4) should therefore be reasonable. A simple one-dimensional heat balance for radial heat transfer through the pipe wall gives

$$h_i = \frac{-\rho_s C_s A_t}{P_i(T - T_g)} \frac{dT}{dt} + \frac{h_o P_o (T_\infty - T)}{P_i (T - T_g)}, \tag{4}$$

where $\rho_s C_s$ is the heat capacity of the pipe wall, A_t is the cross-sectional area of the pipe wall, P_i is the inner periphery of the pipe, T is the measured wall temperature (assumed constant through the pipe wall), T_g is estimated or measured gas temperature, dT/dt is the time rate of change of the wall temperature obtained by curve fit of the measured

temperature, h_o is the heat transfer coefficient on the pipe outside, P_o is the outer periphery of the pipe and T_∞ is the air temperature. The result of using Eq. (4) is compared with the heat transfer coefficients used by PIA in Fig. 6. In the beginning, dT/dt is zero because the cold front has not reached the outer wall surface and the simplified analysis does not apply in this area. The estimates of h_i are valid after about 60 s. The two estimates of h_i using Eq. (4) is based on the measured gas temperature upstream of the nozzle and the measured gas temperature minus 10 °C to use a gas temperature closer to the estimate given by PIA. For the other cross-sections similar results are obtained and the heat transfer coefficient is reduced from a maximum of about 100–150 W/m^2 K to about 20–30 W/m^2 K during the depressurization. The outer wall temperature is a mean temperature for all the measured temperatures in a cross-section except for the top point (point 5) for vertical cross-sections. The maximum deviation between calculated h_i and estimates based on the experiments using a simplified model, is in the area of ± 20 to $\pm 30\%$. This is about the same as the uncertainty experienced in using the empirical expressions for h_i as in PIA.

5. Conclusions

A comparison is made between measurements and simulations of blow-down of a riser platform. Calculations of outer pipe wall temperatures are in good agreement with measurements. The simulations are however 1D and 2D, and 3D effects are not taken care of by the present version of the code PIA. The measured temperatures will vary in a cross-section giving smaller temperature decreases on the top of horizontal pipes. Estimations of the heat transfer coefficients involved using a simplified analysis produces results that are in agreement with the estimates made by the simulation code. For practical engineering purposes, PIA seems to give satisfactory results for gas systems with not too much liquid present by use of conventional heat transfer expressions in a 1D and 2D grid system.

Acknowledgements

The measurements were performed together with Erling Mikkelsen. His participation is gratefully acknowledged.

References

[1] B.T. Arnberg, J. Basic Eng. Trans. ASME, 84 (1962) 447.
[2] Installation guide, 3595 series isolated measurement pods, Schlumberger Technologies.
[3] Operating manual, 35954A IMP/PC to S-net adaptor, Schlumberger Technologies.
[4] Altair DOS version users guide, version 2.15, Dickinson Control Systems.
[5] Cypros users guide, Camo A/S.
[6] T. Evanger, J.A. Fagertun, T.E. Hals, B.F. Magnussen and T. Strøm, PIA – A computer program system for depressurization analysis, Sintef Report STF15 F88011, 1988.
[7] F.P. Incropera and D.P. DeWitt, Fundamentals of Heat and Mass Transfer, 3rd edn., Wiley, New York, 1990.